

Statistical Mechanics of Histories: A Cluster Monte Carlo Algorithm

Natali Gulbahce, Francis J. Alexander, Gregory Johnson
*Los Alamos National Laboratory, P.O.Box 1663,
Los Alamos, NM, 87545.*

We present an efficient computational approach to sample the histories of nonlinear stochastic processes. This framework builds upon recent work on casting a d -dimensional stochastic dynamical system into a $d+1$ -dimensional equilibrium system using the path integral approach. We introduce a cluster algorithm that efficiently samples histories and discuss how to include measurements that are available into the estimate of the histories. This allows our approach to be applicable to the simulation of rare events and to optimal state and parameter estimation. We demonstrate the utility of this approach for ϕ^4 Langevin dynamics in two spatial dimensions where our algorithm improves sampling efficiency up to an order of magnitude.

I. INTRODUCTION

Onsager and Machlup [1] pioneered the path ensemble approach to classical stochastic processes in 1953, only a few years after Feynman's seminal work on quantum systems [2]. Despite nearly simultaneous origins however, the computational application of this framework to classical systems lagged far behind its quantum counterpart. While Monte Carlo methods were applied to lattice gauge theory and quantum condensed matter systems in the early 1970's [3], only within the past decade has the Onsager-Machlup approach become practical for computational modelling of classical nonequilibrium processes.

Following the analytical results of Domany [4] for 2+1 dimensional Potts models, computational work began with Zimmer [5] who devised a Monte Carlo algorithm to sample entire space-time configurations, or histories, of a kinetic Ising model. This work demonstrated the utility of the Monte Carlo approach where histories can be conditioned on rare events. Olender and Elber [7] used a similar approach to circumvent the time limitations of molecular dynamics simulations, specifically to find reaction pathways when both the initial and final states are known. See the work of Chandler et al. [6], Jónsson et al. [8] and others using this methodology [9, 10].

In this paper we extend the computational work by presenting a percolation-based cluster Monte Carlo approach to sample the statistical mechanics of histories for nonlinear stochastic processes. We also describe how to apply this method to rare event simulations and optimal estimation. The cluster algorithm we present improves the statistical sampling of histories in Monte Carlo simulations significantly. In traditional spatial cluster algorithms [11], the clusters represent statistically independent objects at a given time. In the $d+1$ dimensional mapping we introduce, the clusters can be interpreted as statistically independent objects in space-time.

Our goal is to determine the conditional statistics of histories for a stochastic dynamical system $\mathbf{x}(t)$, given a model and incomplete information about that system. The state vector \mathbf{x} satisfies the following Itô process:

$$d\mathbf{x}(t) = \mathbf{f}(\mathbf{x}, t)dt + (2\mathbf{D}(\mathbf{x}, t))^{1/2}d\mathbf{W}(t), \quad (1)$$

where $\mathbf{f}(\mathbf{x}, t)$ is the force term, and the stochastic effects are provided by the last term, in which the diffusion matrix \mathbf{D} acts on a vector-valued Wiener process, \mathbf{W} . We assume that the noise errors are uncorrelated, and that the initial value $\mathbf{x}(t_0)$ is a random variable with a known distribution. This system could represent the configuration of a protein evolving under Brownian dynamics [7], the concentration of interacting metabolites, the locations of atoms in a crystal undergoing a structural phase transition or nucleation, or the state of a queue in a stochastic fluid model. The final state can also be a rare event on which the history is conditioned. For instance, the configuration of an unfolded protein chain can be conditioned in the initial state and the folded protein in the final state.

The probability of the dynamics generating a given history is simply related to the probability that it experiences a certain noise history, $\eta(t_k) \equiv \mathbf{W}(t_{k+1}) - \mathbf{W}(t_k)$, at times t_k , where $k = 0, 1, \dots, T$. We incorporate this probability into the discretized form of Eq. (1). In the interest of simplicity, we use the explicit Euler-Maruyama discretization scheme. This leads to the following:

$$\mathbf{x}_{k+1} = \mathbf{x}_k + \mathbf{f}(\mathbf{x}_k, t_k)\Delta t + (2\mathbf{D}(\mathbf{x}_k, t_k))^{1/2}\eta(t_k). \quad (2)$$

For Gaussian uncorrelated white noise with variance $\langle \eta \eta' \rangle = \delta(t - t')$, the probability distribution of noise is $P\{\eta(t)\} \propto \exp(-\frac{1}{2} \sum_k |\eta(t_k)|^2 / \Delta t)$. The probability of a specific history is given by, $P\{\eta(t)\} \propto \exp(-S)$ where S is the action of the d -dimensional system (equivalent to the Hamiltonian of the $d+1$ -dimensional system). By rearranging terms in Eq. 2, the form of the action becomes

$$S \equiv \sum_{k=0}^{T-1} \frac{1}{4\Delta t} \left\{ [\mathbf{x}_{k+1} - \mathbf{x}_k - \mathbf{f}(\mathbf{x}_k, t_k)\Delta t]^\top \mathbf{D}(\mathbf{x}_k, t_k)^{-1} [\mathbf{x}_{k+1} - \mathbf{x}_k - \mathbf{f}(\mathbf{x}_k, t_k)\Delta t] \right\} \quad (3)$$

where \top indicates the transpose. With action S , the statistics of histories of the time dependent, stochastic dynamical system has been cast as an equilibrium statistical mechanical system.

Now let us incorporate the information about the system into the action functional. For simplicity, we will

assume that the information comes at discrete times t_m where m labels each observation $m = 1, \dots, M$. These observations (e.g. experimental measurements) are given in a function, $\mathbf{h}(\mathbf{x}, t)$, and it is assumed to have errors denoted here by $\epsilon(\mathbf{x}, t)$, i.e.,

$$\mathbf{y}(\mathbf{x}_m, t_m) = \mathbf{h}(\mathbf{x}_m, t_m) + \epsilon_m,$$

with error covariance, $\langle \epsilon \epsilon' \rangle = \mathbf{R}_m$. By using Bayes' rule [10], the action arising from measurements becomes

$$S_M = \sum_{m=1}^M (\mathbf{h}_m - \mathbf{y}_m)^\top \mathbf{R}_m^{-1} (\mathbf{h}_m - \mathbf{y}_m). \quad (4)$$

The action-functional, $S_{\text{total}} = S + S_M$, assigns weights to individual histories. In the absence of additional information, histories unlikely to arise from the dynamics are given a lower weight than histories which are more likely. However, when there are measurements, histories which are far from the measurements are given lower weight than those closer to the measurements.

II. A SPACE-TIME CLUSTER ALGORITHM

To sample the distribution of histories and hence to assign weights to them, various methods have been applied (including local Monte Carlo, unigrid and generalized hybrid Monte Carlo [10]). Here we describe a space-time cluster algorithm which is an extension of the embedded dynamics algorithm introduced by Brower and Tamayo (BT) [14]. Cluster algorithms are widely used in physics, statistics and computer science [13]. The first of these was introduced by Swendsen and Wang (SW) [11] which is based on a mapping between the Potts model and a percolation problem [12].

Brower and Tamayo extended the SW algorithm to a continuous field theory by embedding discrete variables (spins) into the continuous field in an equilibrium classical ϕ^4 model [14]. The ϕ^4 potential is a symmetric double well potential of the form:

$$V(\mathbf{r}, t) = (a/4)\phi^4(\mathbf{r}, t) - (b/2)\phi^2(\mathbf{r}, t) \quad (5)$$

The discrete spin variables, s_r , label the two wells in ϕ^4 potential such that $\phi_r = s_r |\phi_r|$. At fixed values of $|\phi(\mathbf{r})|$ a ferromagnetic Ising model is embedded into the ϕ^4 field theory which allows the use of the SW dynamics. The detailed procedure of the embedded dynamics is as follows:

- Update ϕ_r via a standard local Monte Carlo algorithm.
- Form percolation clusters dictated by the bond probability,

$$p_{rr'} = 1 - e^{-\beta_{rr'}(1+s_r s_{r'})} = 1 - e^{-(|\phi_r| |\phi_{r'}| + \phi_r \phi_{r'})},$$

where the effective spin-spin coupling is $\beta_{rr'} = |\phi_r \phi_{r'}|$. Note that $p_{rr'}$ reduces to $1 - \exp(-2\beta_{rr'})$ when the spins

are the same sign.

- Update the Ising variables by flipping the percolation clusters independently with probability 1/2. If the move is accepted, flip the sign of the fields in the cluster.

To extend the embedded dynamics to space-time, we need to redefine the clusters based on the discretized dynamical equation and the corresponding action as in Eqs. 2 and 3. Next we illustrate this formalism with the ϕ^4 field theory in (2 + 1) dimensions.

We consider the discretized Langevin equation,

$$\begin{aligned} \phi(\mathbf{r}, t + \Delta t) = & \phi(\mathbf{r}, t) + \frac{\Delta t}{\Delta x^2} \left[\sum_i \phi(\mathbf{r}_i, t) - 4\phi(\mathbf{r}, t) \right] \\ & + \Delta t [-a\phi(\mathbf{r}, t)^3 + b\phi(\mathbf{r}, t)] + \sqrt{\Delta t} \eta(\mathbf{r}, t), \end{aligned} \quad (6)$$

where the force term is the derivative of Eq. 5 with respect to ϕ , and \sum_i is sum over the nearest neighbors of $\phi(\mathbf{r}, t)$. The noise variables $\eta(\mathbf{r}, t)$ are chosen to be Gaussian distributed, independent random variables of mean zero and with correlations $\langle \eta(\mathbf{r}, t) \eta(\mathbf{r}', t') \rangle = 2D \delta_{\mathbf{r}, \mathbf{r}'} \delta(t - t')$. For this model the action becomes

$$\begin{aligned} S \equiv & \frac{1}{4D\Delta t} \sum_{r,t} \left(\phi(\mathbf{r}, t + \Delta t) - \phi(\mathbf{r}, t) - \Delta t [-a\phi^3(\mathbf{r}, t) \right. \\ & \left. + b\phi(\mathbf{r}, t)] - \Delta t \left[\sum_i \phi(\mathbf{r}_i, t) - 4\phi(\mathbf{r}, t) \right] \right)^2. \end{aligned} \quad (7)$$

By expanding the square in the right side of Eq. 7, we obtain many cross terms representing different couplings between neighbors both in space and time. All of the interactions between a site and its neighbors in space and time are shown explicitly by Zimmer [5]. Excluding the local terms (e.g. $\phi(\mathbf{r}, t)^2$), the interactions yielding different spin-spin couplings can be grouped into four types (using (\mathbf{r}_j, t_k) as the reference site):

1. Nearest neighbors of (\mathbf{r}_j, t_{k-1}) coupled to (\mathbf{r}_j, t_k) :

$$\beta_1 = 2\Delta t \left(\sum_i \phi(\mathbf{r}_i, t_{k-1}) \right) \phi(\mathbf{r}_j, t_k).$$

2. Site (\mathbf{r}_j, t_{k-1}) coupled to (\mathbf{r}_j, t_k) :

$$\beta_2 = \left[(2b-8)\Delta t - 2a\Delta t \phi^2(\mathbf{r}_j, t_{k-1}) + 2 \right] \phi(\mathbf{r}_j, t_k) \phi(\mathbf{r}_j, t_{k-1}).$$

3. Nearest neighbors of (\mathbf{r}_j, t_k) coupled to each other:

$$\beta_3 = -\Delta t^2 \left(\sum_i \phi(\mathbf{r}_i, t_k) \right) \left(\sum_i \phi(\mathbf{r}_i, t_k) \right).$$

4. Nearest neighbors of (\mathbf{r}_j, t_k) coupled to (\mathbf{r}_j, t_k) :

$$\begin{aligned} \beta_4 = & \left(\sum_i \phi(\mathbf{r}_i, t_k) \right) \left([(8-2b)\Delta t^2 - 2\Delta t] \phi(\mathbf{r}_j, t_k) \right. \\ & \left. + 2a\Delta t^2 \phi^3(\mathbf{r}_j, t_k) \right). \end{aligned}$$

The probability of a site having a bond with any of its neighbors is

$$P_i = 1 - e^{-2\beta_i/(4D\Delta t)}, \quad (8)$$

where $i = 1, \dots, 4$. A significant difference from BT is that the sign of β_i is not known *a priori*. Depending on the value of ϕ , the interaction can be either ferromagnetic or antiferromagnetic [15]. At each step we determine whether the coupling term is ferromagnetic ($\beta_i > 0$) or antiferromagnetic ($\beta_i < 0$) and require the signs of spins to be the same or opposite respectively for a bond to exist. Once the clusters are defined, we use the same steps as BT described earlier in text.

Next, we compare the performance of this cluster method to two other algorithms, local Monte Carlo and unigrid [10]. To quantify performance, we measured the correlation time of a quantity $M = |\sum \phi|$, the sum of fields at all space and time points. This quantity is analogous to the magnetization of a spin system. Because M is a global quantity, it is one of the slowest modes of the system [16]. We remind the reader that our cluster algorithm updates the fields by changing the sign of fields in a flipped cluster. Therefore, by taking the absolute value of the fields we are left with the true correlations. The correlation time, τ , is obtained by fitting $\exp(-t/\tau)$ to the autocorrelation function defined as $\langle M_{t_0+t} M_{t_0} \rangle$.

TABLE I: Correlation times of the magnetization M for local and cluster algorithms for several noise strengths, D . The system dimensions are $L = 10$ and $T = 100$, the acceptance ratio, $a \approx 0.5$, $\Delta t = 0.05$ and $\Delta x = 1.0$. The length of the run was 100,000 MCS, and the data analyzed for the last 80,000 MCS. The cluster algorithm is fastest at $D \approx 25$.

D	τ_{local}	$\tau_{cluster}$
1	947	775
5	180	134
15	25	8.8
20	19	2.9
25	12	1.4
30	9	1.1

The performance of the cluster algorithm depends on several factors. For a fair comparison of our algorithm to the local one, we used an acceptance ratio of $a \approx 0.5$ for which the local algorithm is empirically most efficient. The correlation times are highly dependent on noise strength (proportional to the square of the temperature) as is expected from any algorithm. We measure τ 's at different noise strengths for a system of spatial dimension, $L = 10$ with periodic boundary conditions and time dimension, $T = 100$ with open boundary conditions. In Table I, these times are shown for the local and cluster algorithms as characterized by the decay of $C_M(t)$. The cluster algorithm performs only slightly better than the local algorithm at low noise strengths, and it is most beneficial at $D \approx 25$ with nine times more efficiency. At this noise strength, the cluster size distribution scales as $n_s \sim s^{-2.2}$ as shown in Fig. 1.

We also compared the performance of the cluster algorithm to a unigrid algorithm [10] which has been shown to speed up the dynamics significantly. In Table II, we

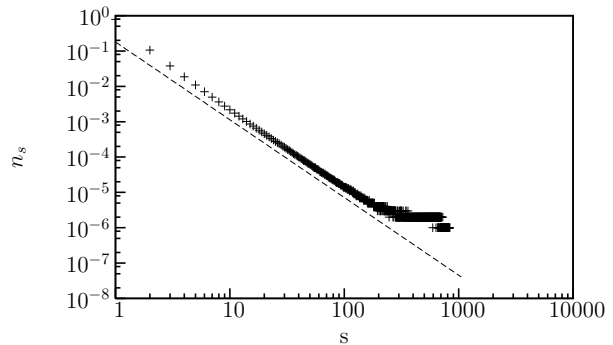


FIG. 1: The cluster size distribution at noise $D = 25$. The size distribution scales as $n_s \sim s^{-2.2}$.

show the performance of the local, cluster and unigrid algorithms at the same noise strength ($D = 25$) for different system sizes. The cluster algorithm correlation times are much smaller than the local τ 's and comparable to the unigrid algorithm.

TABLE II: Correlation time, τ , of magnetization, M , with the local, cluster and unigrid algorithms for different system sizes, L and T with $D = 25$. The cluster algorithm is a factor of nine faster than the local one, and comparable to unigrid.

L	T	τ_{local}	$\tau_{cluster}$	$\tau_{unigrid}$
8	32	12.2	1.74	1.54
16	128	11.1	1.50	1.80
32	512	13.3	1.79	1.62

III. MEASUREMENTS

Thus far we have not included any measurements or local fields in the system. In forecasting complex systems (e.g. weather) it is crucial to make use of data available to predict the path of the system. The cluster algorithm we have introduced is especially useful where some measurements are available. As illustrated in Eq. 3, the action corresponding to the measurements, S_M , can be added to the action, S , in Eq. 7:

$$S_M = \sum_m \frac{[\phi(\mathbf{r}_m, t_m) - \phi_m(\mathbf{r}_m, t_m)]^2}{2\sigma_m^2}, \quad (9)$$

where ϕ_m is the value of ϕ measured at \mathbf{r}_m, t_m with error variance σ_m^2 . The cluster algorithm can be easily modified to incorporate the measurements. The spin-spin couplings defined earlier remain the same because the measurements are added to the action separately and are independent of the dynamics. However the cluster flipping probability must be adjusted since it costs more/less to flip the sign of a spin if there is a measurement at that point. The local field at a site is analogous to having a

measurement in our case. Dotsenko et al. [17] have discussed the probability of flipping a site in an Ising model when there are local fields at that site. In the presence of external field h , the probability of flipping a cluster gets weighted by the local fields, i.e.,

$$p_{\text{flip}} = \exp(\pm \sum_j h_j) / [\exp(\sum_j h_j) + \exp(-\sum_j h_j)], \quad (10)$$

which reduces to $p_{\text{flip}} = 1/2$ as expected for $h = 0$.

Let us now derive the probability of flipping a cluster in the presence of measurements. Expanding the square in the right hand side of the action in Eq. 9 yields only one coupled term, $-2\phi(\mathbf{r}_m, t_m)\phi_m(\mathbf{r}_m, t_m)$. With this coupled term, the flipping probability becomes

$$p_{\text{flip}} = \frac{e^{\sum_m -2\phi(\mathbf{r}, t)\phi_m(\mathbf{r}, t)}}{e^{\sum_m 2|\phi(\mathbf{r}, t)|\phi_m(\mathbf{r}, t)} + e^{\sum_m -2|\phi(\mathbf{r}, t)|\phi_m(\mathbf{r}, t)}}. \quad (11)$$

We set artificial measurement points such that the system is initially in the positive well (at $t = 0$), and it transitions into the negative well forced by the measurements. We measured the probability distribution function (pdf) of ϕ using the cluster algorithm as shown in Fig. 2. The pdf obtained using the local algorithm agrees with this pdf as expected. In Table III, we show the performance of both algorithms for different system sizes ($D = 25$) with four measurements points of variance $\sigma^2 = 0.01$. The cluster algorithm consistently outperforms the local algorithm in the presence of the measurements.

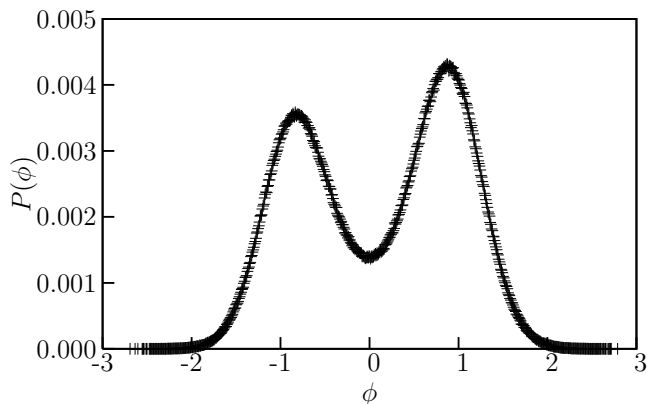


FIG. 2: Probability distribution function pf ϕ obtained by the cluster algorithm. The system is $L = 10$, $T = 20$, and $D = 1$ with measurement points, ϕ_m , placed at every space point at every three time slices, $\phi_m(t < T/2) = 1$ and $\phi_m(t > T/2) = -1$ with a standard deviation of $\sigma = 0.02$. The system is driven to the negative well forced by the measurements.

IV. DISCUSSION

In this paper, we have described a cluster Monte Carlo algorithm to sample space-time histories of a nonlinear

TABLE III: Correlation times of M for local and cluster algorithms with measurements at different system sizes at noise strength, $D = 25$. The cluster algorithm consistently outperforms the local one.

L	T	τ_{local}	τ_{cluster}
8	32	10.8	1.7
12	72	11.3	1.6
16	128	11.9	1.5
24	288	12.3	1.7

stochastic process. This approach can be applied to study pathways to rare events as well as for optimal state and parameter estimation.

At the noise strength where the cluster size distribution scales, the cluster algorithm outperforms the local Monte Carlo updates significantly. We have not observed scaling of magnetization correlation times as a function of system size, therefore the observed speedup is independent of the system size. The noise strength required to observe this scaling depends on the size of the space-time domain. For the finite (and relatively small) systems we have studied in this paper, this noise does not correspond to the critical temperature in the original D dimensional system.

Although the efficiency of our algorithm is comparable to the unigrid algorithm, it can be preferred over the unigrid method when the observation of the clusters as correlated structures is of interest. The clusters are statistically independent space-time events, and the temporal (time-axis) extent of these objects provides an estimate of their lifetime. For instance in nucleation process, the correlated structures in the system, e.g. droplets, signify the fluctuations of the metastable equilibrium [18] and it is of interest to measure the lifetime of these droplets directly. In the future we plan to use this method to simulate the Ginzburg-Landau equation (model A) in order to study nucleation and find the distribution of the lifetimes (τ) of clusters to test theoretical predictions [18].

Our method is applicable to more general potentials arising from other nonlinear stochastic partial differential equations such as Cahn-Hilliard-Cook equation which enables the study of spinodal decomposition.

Acknowledgments

We thank G. L. Eyink, W. Klein, J. Machta, and S. K. Mitter for useful discussions. This work (LA-UR 05-8402) was funded partly by the Department of Energy under contracts W-7405-ENG-36 and the DOE Office of Science's ASCR Applied Mathematics Research program, and partly by Center for Nonlinear Studies.

-
- [1] L. Onsager and S. Machlup, Phys. Rev. **91**, 1505 (1953).
L. Onsager, Phys. Rev. **38**, 2265 (1931).
- [2] R. P. Feynman and A. R. Hibbs, *Quantum Physics and Path Integrals*, New York: McGraw-Hill, (1965).
- [3] J. B. Kogut, Rev. Mod. Phys. **51**, 659 (1979). M. Suzuki, Prog. Theor. Phys. **56**, 1454 (1976). H. F. Trotter, Proc. Am. Math. Soc. **10**, 545 (1959).
- [4] E. Domany, Phys. Rev. Lett. **52**, 871 (1984).
- [5] M. F. Zimmer, Phys. Rev. Lett. **75**, 1431 (1995).
- [6] C. Dellago, P. Bolhuis, F. Csajka, and D. Chandler, J. Chem. Phys. **108**, 1964 (1998).
- [7] R. Olender and R. Elber, J. Chem. Phys. **105**, 9299 (1996).
- [8] H. Jónsson, G. Mills and K. W. Jacobsen, *Classical and Quantum Dynamics in Condensed Phase Simulations*, (World Scientific, Singapore, 1998).
- [9] W. E, W. Ren, and E. Vanden-Eijnden, Phys. Rev. B **66**, 52301 (2002). D. M. Zuckerman and T. B. Woolf, Phys. Rev. E **63**, 016702 (2000). D. Passerone and M. Parrinello, Phys. Rev. Lett. **87**, 108302 (2001). R. J. Allen, D. Frenkel, P. R. ten Wolde, cond-mat/0509499 (2005).
- [10] F. J. Alexander, G. L. Eyink and J. M. Restrepo, J. Stat. Phys. **119**, 1331 (2005).
- [11] R. H. Swendsen and J.-S. Wang, Phys. Rev. Lett **58**, 86 (1987).
- [12] C. M. Fortuin and P. W. Kasteleyn, Physica **57**, 536 (1972).
- [13] A. Barbu and S. C. Zhu, IEEE Trans. PAMI (2005).
- [14] R. C. Brower and P. Tamayo, Phys. Rev. Lett. **62**, 1087 (1989).
- [15] J.-S. Wang, R. H. Swendsen and R. Kotecký, Phys. Rev. Lett. **63**, 109 (1989).
- [16] R. Toral, in *Third Granada Lectures in Computational Physics: Proceedings of the III Granada Seminar on Computational Physics*, (Springer-Verlag, Berlin, 1995).
- [17] V. I. S. Dotsenko, W. Selke and A. L. Talapov, Physica A **170**, 278 (1991).
- [18] C. Unger and W. Klein, Phys. Rev. B **29**, 2698 (1984).